*Journal of The Electrochemical Society*, **148** (5) C369-C375 (2001)
0013-4651/2001/148(5)/C369/7/$7.00 © The Electrochemical Society, Inc.


# Effect of the Electrosynthesis Method on the Surface Morphology of the Polypyrrole Film

## An Atomic Force Microscopy Study

**T. Hernández-Pérez,[a,*] M. Morales,[b] N. Batina,[b**] and M. Salmón[a,z]**

[a]*Instituto de Química, Universidad Nacional Autónoma de México, 04510 México D.F., México*
[b]*Departamento de Química, Universidad Autónoma Metropolitana-Iztapalapa, 09340 México D.F., México*

The surface morphology of polypyrrole (ppy) films prepared by potentiostatic and voltammetric methods at the platinum electrode was studied by *ex situ* atomic force microscopy (AFM). The study was mainly focused on the early stages of polymer film growth up to a film thickness of 30 to 50 nm. AFM analysis revealed that polymer film morphology depends on the electrosynthesis method used. Electrosynthesized films produced by the voltammetric method consisted of nano-size ppy nodules, which during the polymer oxidation process become associated forming larger surface aggregates. However, in thicker films and those prepared using a large anion, this association was not observed. The ppy films formed by the potential step method (potentiostatic) allowed a better control of the early stages of the electropolymerization process. Thus, the AFM study showed that the first ppy nodules grow three-dimensionally during the application of the potential pulse steps, and simultaneously their number increase on the electrode surface according to the progressive nucleation and growth model. Negligible association of ppy nodules was noticed for the film prepared by the potentiostatic method, which suggests that this synthesis method is a better alternative for controlling ppy film growth.
 [DOI: 10.1149/1.1365143] 

Manuscript submitted September 6, 2000; revised manuscript received January 29, 2001.

Conducting polymeric films of polypyrrole (ppy) have been examined for their possible applications in electronics, batteries, electrochromic devices, selective membranes, sensors, and capacitors, among others.[1-5] The quality and properties (including conductivity) of the electrochemically synthesized ppy films depend on many different factors, *e.g.*, doping anion, electropolymerization method (potentiostatic, galvanostatic, or voltammetric), selected solvent, and the electrode substrate.[6-9] It has been known for sometime that, depending on the electrochemical polymerization conditions, the electrosynthesized ppy film could possess different surface morphology characteristics, which have an impact on the polymer film properties.[7,10-12]

In previous studies the surface morphology of ppy films was mainly visualized by scanning electron microscopy (SEM).[10,11,13,14] Recently, the novel microscopies, scanning tunneling microscopy (STM) and atomic force microscopy (AFM) have been implemented for polymer film studies.[9,14,15-26] The surface morphology of the ppy film was analyzed using different electrosynthesis preparation conditions, doping states, and mechanisms of growth. In general, ppy films are amorphous. However, in some isolated experiments it was also found that a small portion of the polymer film can be semicrystalline exhibiting a helical structure.[16]

Among many other findings, it is interesting to mention that Li and Wang,[19] using AFM and STM, found a correlation between the ppy film surface morphology and its thermal stability, as well as its ionic conductivity.[19,21] They also reported a difference in the morphology of the oxidized and the reduced states of the ppy film. Indeed, they postulated that the ionic film conductivity is determined by differences in its surface morphology.[21] Naoi *et al.*[27] used SEM and AFM to study the growth of a ppy film on an indium tin oxide (ITO) electrode in the presence of different surfactant anions as dopants. In this case, they observed the formation of columnar structures of the ppy films. In turn, Kaynak *et al.*[22] found that low doped semiconducting polymer films usually possess a smoother surface morphology, whereas highly doped conducting films develop a dendrite-type surface. The polymer films used in their research were 10 to 200 μm thick.

Recent studies showed that the morphology and other ppy film properties are also functions of the film thickness. Silk *et al.*[23] studied the surface morphology for film thicknesses ranging between 100 and 4000 nm. Those films were prepared by a potentiostatic electropolymerization method using an electrolyte with four different doping anions ($Cl^-$, $ClO_4^-$, $SO_4^{2-}$, and dodecylsulfate). In films with thickness below 1000 nm, a slight influence of the doping anion on the polymer surface morphology was found. However, for thicker films, a significant difference on some surface characteristics (average diameter, height, and shape) was found for the different anions examined.[24]

An attempt to examine the influence of the electrosynthesis method (voltammetric *vs.* potentiostatic) on the surface morphology of the ppy film was made by Yang *et al.*[25] However, the quality of the AFM images did not allow them to draw definitive conclusions.

Suares and Compton[9] recently described the relationship between the electrosynthesis conditions and the final polymer film structure and morphology. The description was based on *in situ* AFM observation of the surface morphology of ppy films prepared by the potentiostatic method. Electrosynthesis was carried out in an aqueous solution, using three different substrates, platinum, glassy carbon, and gold electrodes. The obtained results showed that the initial polymer film growth (thickness between 25 and 1000 nm) depends on both the supporting electrolyte and the electrode material (Au *vs.* Pt).

In contrast to the Suares and Compton work,[9] in the present study, ppy films were prepared in nonaqueous solutions (acetonitrile) using the potentiostatic and voltammetric methods. The polymer films were prepared on a polycrystalline platinum electrode using either tetrafluoroborate or *p*-toluenesulfonate as doping anions.

The major aim of this work is to investigate the influence of the electrosynthesis conditions on the quality and surface morphology of ppy film formation as well as the influence of redox style of the polymer. The study is mainly focused on the early stages of the polymer film growth, where the film thickness was 5 or 30 nm. The surface morphology was examined by *ex situ* AFM.

### Experimental

*PPY film preparation.*—The ppy films were prepared by pyrrole (Py) electropolymerization in acetonitrile solution (0.0016 and 0.22 M) containing 0.1 M tetraethylammonium tetrafluoroborate ($Et_4NBF_4$). In order to study the influence of different anions on the

* Electrochemical Society Student Member.
** Electrochemical Society Active Member.
z E-mail: salmon@servidor.unam.mx

polymer film morphology, the film was also prepared in acetonitrile solution containing 0.075 M tetrabutylammonium *p*-toluenesulfonate (TBA*p*-TS) and 0.0016 M of Py monomer. Two different electrochemical methods were used for the ppy electrosynthesis, cyclic voltammetry (voltammetric method) and potential step chronoamperometry (potentiostatic method). In all the electrochemical experiments a three-electrode electrochemical cell was used with a Pt film supported on glass with an electrode area of 0.25 $cm^2$ as the working electrode, a Pt gauze (area 4 $cm^2$) as the counter electrode, and Ag/0.1 M $AgBF_4$ as the reference electrode. All potentials are referred to the Ag/0.1 M $AgBF_4$ electrode. The experiments were performed in an inert atmosphere after careful deoxygenation of the electrochemical cell with super pure $N_2$ (15 min). Both voltammetric and potentiostatic ppy film deposition were carried out by means of an EG&G PAR 173 potentiostat-galvanostat (USA), coupled to both an EG&G PAR 175 universal programmer and a Hewlett Packard 7004B X-Y recorder.

*AFM imaging*.—An atomic force microscope (AFM), Nanoscope III, from Digital Instruments (DI, USA), was used to observe the surface morphology of the ppy films under ambient laboratory conditions. Freshly prepared ppy films were examined in their different redox states: oxidized, and reduced. AFM imaging was performed in the contact mode using standard geometry silicon nitride probes provided from DI. Images were collected using a scan rate of 1 Hz, to minimize possible damage of the polymer sample. No significant damage of the polymer surface was observed during the process. Each sample was probed at four different places. Images are presented in the height mode, with higher portions corresponding to bright colors in the image. The 3D image presentation was intentionally used to emphasize morphology differences between polymer film surfaces. Quantitative evaluation of the polymer surface morphology was performed using the software package provided with the Nanoscope III.

*Chemicals and solutions*.—The pyrrole (Py) monomer (Aldrich) was purified by distillation in vacuum before each experiment. Acetonitrile solvent (HPLC grade, Prolabo), TBA*p*-TS, and $AgBF_4$ (Aldrich) were used as received. $Et_4NBF_4$ (Aldrich) was recrystallized and dried in vacuum before using. In order to prepare the working solution, the electrolyte was dissolved in acetonitrile, deoxygenated with superpure nitrogen after the Py monomer was added. All experiments were made the same day, maintaining the Py solution under nitrogen.

## Results and Discussion

*PPY film prepared by the voltammetric method*.—The electrosynthesis of the ppy film was carried out during a single scan in a selective range of the electrode potentials. Cathodic and anodic potential limits were adjusted in such ways that reduced or oxidized films can be monitored independently.

Figure 1 shows a typical cyclic voltammogram of the Py oxidation on the Pt electrode recorded in acetonitrile solution containing 0.1 M $Et_4NBF_4$ and $1.6 \times 10^{-3}$ M of Py. The voltammogram is characterized by an irreversible oxidation peak at +1.0 V, as previously reported by Díaz *et al.*[28] The scan starts at 0.10 V (zero current potential, $E_{I=0}$), and potential changes toward positive limits at a scan rate of 0.1 V/s. To obtain the film at its oxidized state, the potential was stopped at the positive limit. For studying ppy film in the reduced state, a new Pt electrode was used, and the potential was scanned from $E_{I=0}$ to the positive limit, then reversed until the negative limit was reached where the ppy film is reduced.[21] The charge density under the electropolymerization peak, at 1.0 V, was determined to be 9.3 $mC/cm^2$, which leads the ppy film thickness of about 40 ± 1 nm. Since the thickness value is based on literature data which indicates that a charge equal to 240 $mC/cm^2$ corresponds to a polymer film thickness of 1 μm.[29,30]

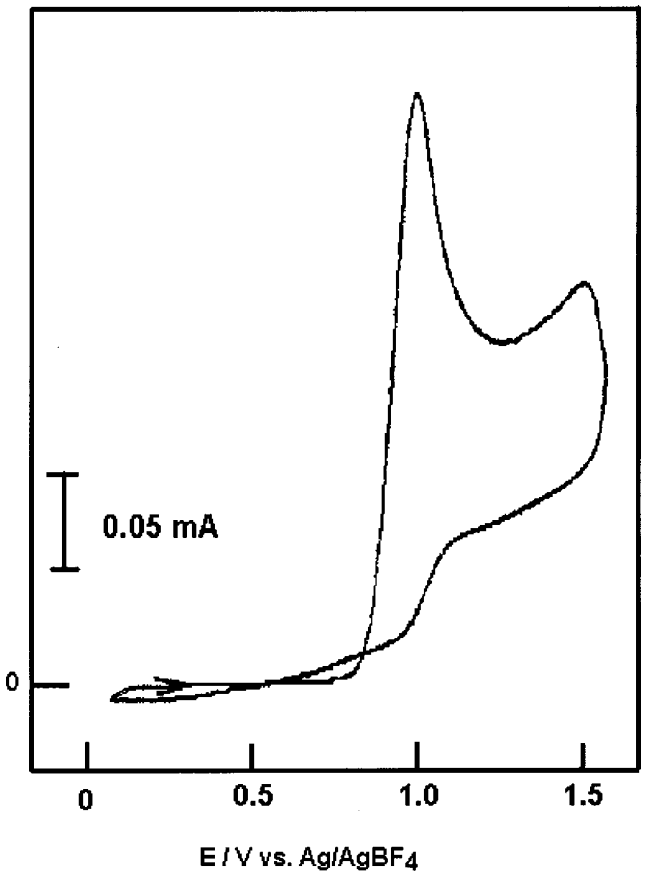


**Figure 1.** Cyclic voltammogram of pyrrole monomer (0.0016 M) oxidation on platinum polycrystalline film electrode using 0.1 M of $Et_4NBF_4$ in acetonitrile solution. Scan started at 0.1 V and coninued toward positive limit using a scan rate of 0.1 V/s.

Figure 2a shows the AFM image of the yellow ppy film in its reduced form.[28-31] The images revealed that the ppy film surface consists of a random distribution of globular features (grains or nodules). The grains were also found associated in pairs or even forming some kind of chain structure, the individual ppy nodules can be easily recognized over the surface, which indicates a weak tendency for the polymer (grain) association. Individual grains are spherical with an average diameter of 40 to 65 nm. A detailed analysis (cross section) shown in Fig. 2b indicates that the bigger grains (B) consist essentially of two associated individual grains (A). Individual grains are 2 nm high, or eventually doubled in size (dimmer grains). Regarding such regularity among the grain shape, size, and height, we suppose that all grains have been formed at the same time (simultaneously), corresponding to the instantaneous form of polymer film nucleation. Figure 2c shows a large scale (4 × 4 μm) AFM image of the ppy film surface, with numerous deep ridges running all over the surface sample in an almost parallel fashion. Individual ppy grains on such a large scale could not be seen, but it is obvious that between such ridges the rest of the surface is very flat.

In order to estimate the surface roughness for the imaged sample, the root-mean-square roughness (rms $[Rq]$) analysis, was performed. The rms $[Rq]$ is a usual parameter to express quantitatively the average surface roughness.[32-36] In 4 μm ppy film samples, the rms $[Rq]$ was found to be 5.0 ± 0.1 nm. However for the smooth portion of the film surface between deep ridges, the rms $[Rq]$ value was found to be much smaller, 1.8 ± 0.1 nm. In order to define the surface morphology of the bare electrode substrate, AFM images of the electrode surface (platinum film deposited on the glass support)

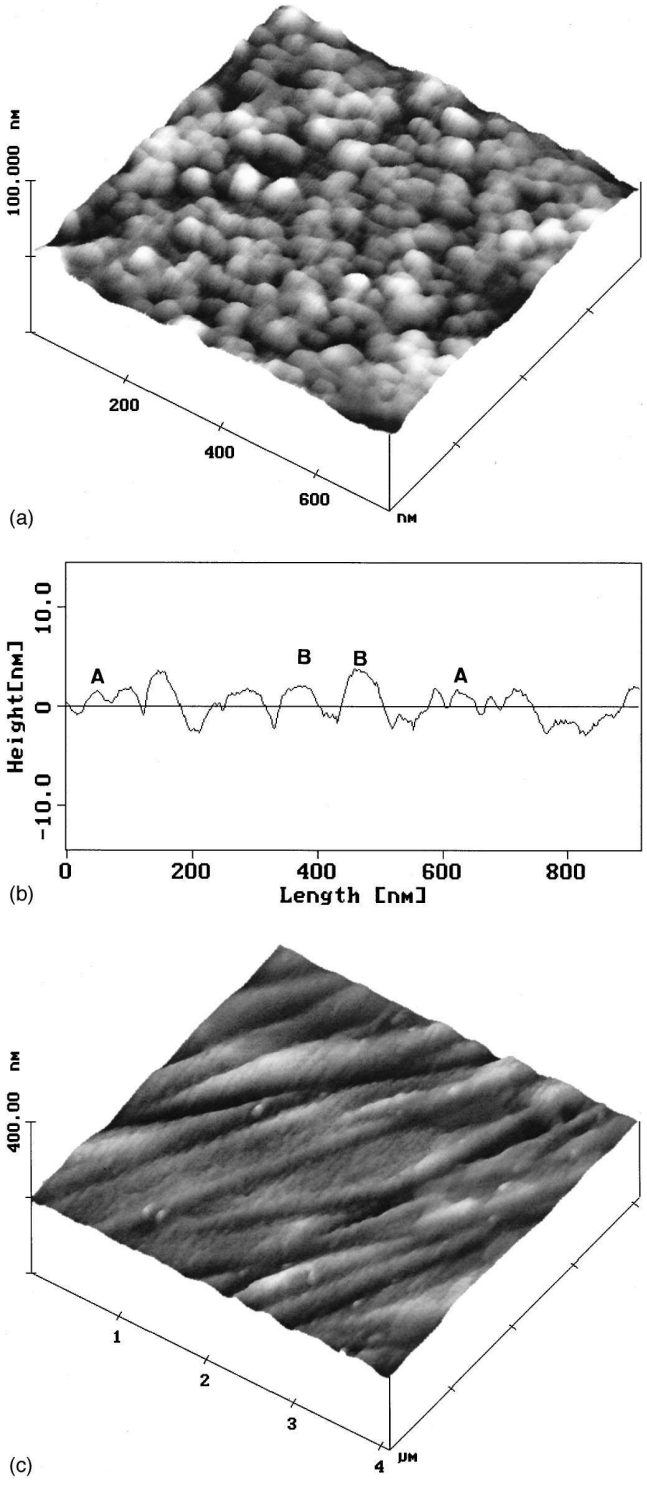


**Figure 2.** (a, top) AFM image of the surface morphology of a ppy film in its reduced state prepared by the voltammetric method, in acetonitrile solution containing 0.1 M $Et_4NBF_4$ and 0.0016 M of pyrrole. During the film preparation the potential was scanned at 0.1 V/s from 0.10 to +1.65 V and switched to 0.10 V. (b, middle) Cross section of the surface area in image (a) showing the morphological characteristics (size, shape, distribution) of the ppy clusters on the polymer film surface. (c, bottom) Large scale of AFM image for ppy film recorded at the same conditions as in (a).

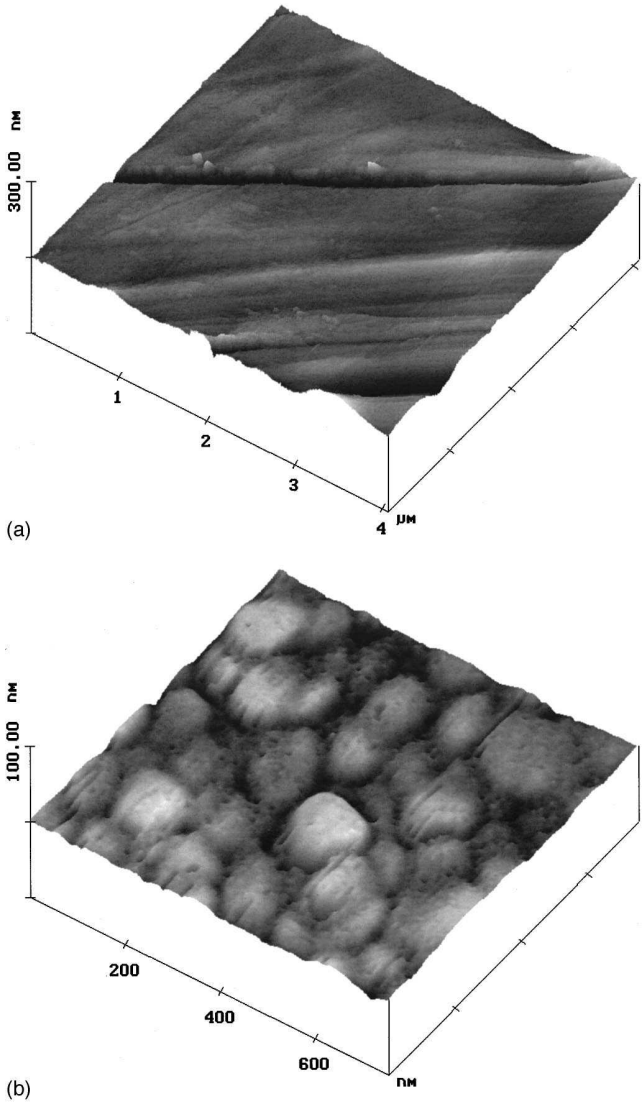


**Figure 3.** Large scale (a, top) and high resolution (b, bottom) AFM images showing the surface of the polycrystalline platinum substrate (Pt film deposited on glass), with typical scratches (ridges) (a) and large platinum grains (b).

were also recorded and evaluated. Note that the pure substrate also possesses deep ridges (see Fig. 3a). The rms $[Rq]$ for the bare Pt surface is $4.7 \pm 0.1$ nm, which is very close to the value obtained for the polymer-coated electrode surface. It shows that electrode was covered with a very thin polymer film, and the main features are related to the platinum substrate morphology. In addition, we also noticed that platinum grains are larger, up to three times (diameter 130 to 170 nm, Fig. 3b) than individual polymer grains. This means that around each substrate grain, three or sometimes four polymer clusters were formed (three to four active sites for ppy electropolymerization reaction on each platinum polycrystalline grain).

Figure 4a shows the AFM image of a ppy film in its oxidized state. It can be observed, that in addition to the numerous individual ppy nodules (as in the reduced state), large features in forms of nonregular patches, were also recognized on the electrode surface. From the shape and morphological characteristics (see the cross section on Fig. 4b), it seems that a new phase was formed via a polymer aggregation process. Although these new features appear to have a smooth surface, the ppy film overall becomes more rough (rms

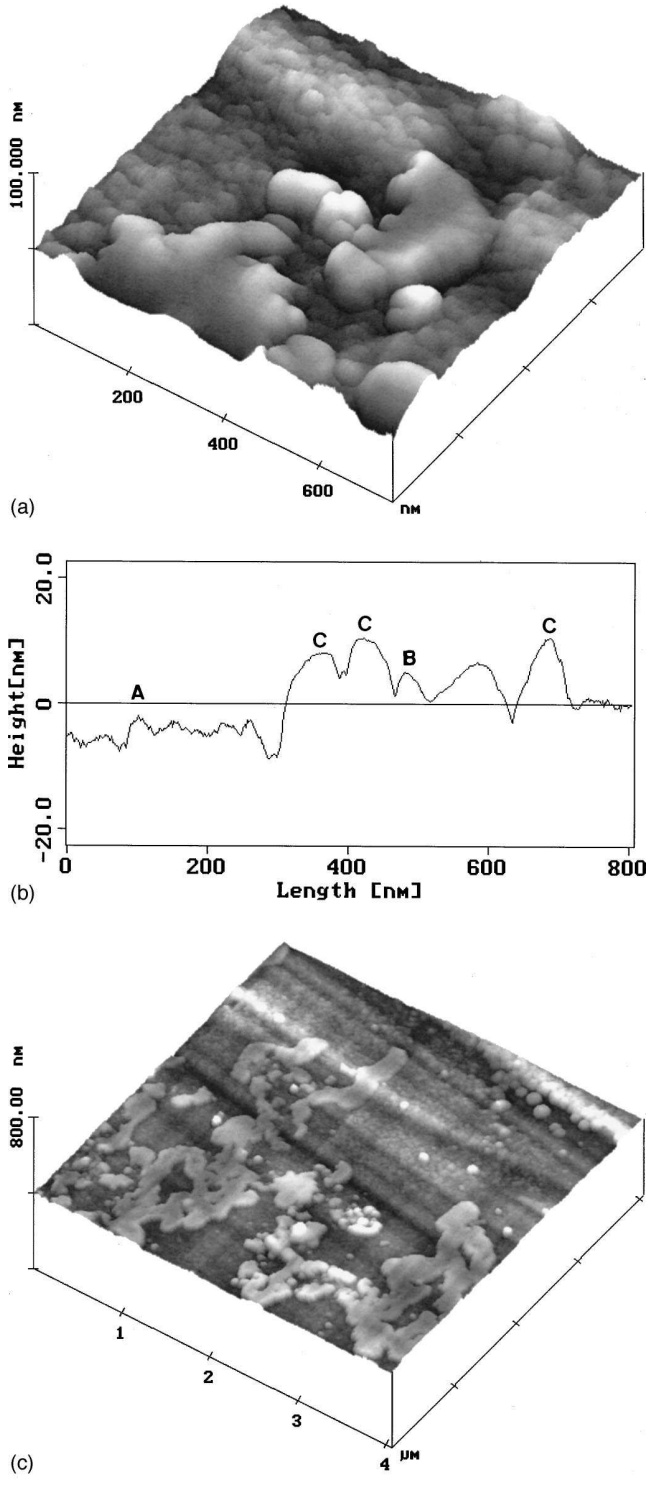


**Figure 4.** (a, top) Characteristic surface morphology of the ppy film in its oxidized state, as revealed by AFM imaging of the film as prepared by the voltammetric method in acetonitrile solution containing 0.1 M $Et_4NBF_4$ and 0.0016 M pyrrole. During the film preparation the potential was cycled at 0.1 V/s from 0.10 to +1.65 V. (b, middle) Cross section taken of image (a) showing the size and shape of a typical features founded on the oxidized ppy film surface. (c, bottom) The AFM image of the ppy film reveals macroscopic size features of the film suface.

$[Rq] = 7.4 \pm 0.1$ nm) and the new phase is evident at the large-scale image shown in Fig. 4c. The observed changes could be the result of the film volume increase, which is due to uptake of anions from solution into the polymer matrix. (Otero *et al.*[31,37,38] have described details of this process previously.) Thus in the oxidized state, the ppy is in the salt form ($ppy^+BF_4^-$) with expanded film volume, whereas in the reduced state, the attractive interactions between the neighboring polymer chains prevail, resulting in a compact and closed polymeric structure.[31,37,38] As oxidation advances, followed by anion incorporation into the polymer matrix, the polymer attractive forces are substituted by strong coulombic repulsion forces between emerging polarons. This leads to an increase in the polymer interchain distances and the polymer film volume. In contrast, Li *et al.*[21] reported that ultrathin ppy films on Au electrode, prepared in aqueous medium (electrolyte *p*-toluenesulfonate) by a voltammetric method, after its oxidation become porous and the micropores serve as channels for achievement of better ionic conductivity.

To investigate the change in the polymer film morphology related to the anion interchange process, we also prepared a ppy film with TBA*p*-TS instead of $Et_4NBF_4$ anion. This is a much larger anion, which could not be easily exchanged between the polymer matrix and the solution. Therefore, it is anticipated, that the anion must remain in the polymer matrix during the polymer redox process. In this case, polymer film reduction is possibly coupled with cation incorporation into the polymer film matrix. According to the recent observation of Suares and Compton,[9] this also leads to an increase in the polymer film volume.

In our experiments, the ppy was prepared by the voltammetric method (−0.50 to 1.30 V) from $1.19 \times 10^{-3}$ M Py solution. Surface morphology of both (reduced and oxidized) forms of ppy film was checked by means of AFM imaging. Surprisingly, images revealed very similar characteristic morphologies for both forms. Grains with diameters of 140 to 150 nm, rms $[Rq]$ *ca.* $2.0 \pm 0.2$ nm, and little evidence for grain association (volume expansion), were found in either form. From these results we can conclude that the ppy film morphology is not strongly perturbed during the cation/anion exchange process.

However, when *p*-TS film was used as the working electrode in a solution containing 0.1 M $Et_4NBF_4$ and the potential was cycled eight times between the positive and negative potentials, some differences between reduced and oxidized forms of the ppy film emerged. The images are similar to those in Fig. 2a and 4a for reduced and oxidized forms of the ppy films, respectively. The experiment demonstrates that changes in the ppy film surface morphology are related to the anion size and anion exchange mechanism between the polymer matrix and the solution. The relation between the anion exchange mechanism and the anion size has been revealed before.[39-41]

On the other hand, the anion size is not the single limiting parameter, which has an influence on the polymer film morphology. Surface morphology is also a function of the polymer film thickness. For example, ppy films prepared from higher Py concentration in the working solution (0.22 M, which is almost 2000 times more than that used in prior experiments), afforded a small difference in the surface morphology between the reduced and the oxidized forms. Although the oxidized polymer film had slightly more associated grains, both forms possess the same rms $[Rq]$ ($69.1 \pm 0.1$ nm). Note that in the case of using 0.22 M instead 0.0016 M of Py, as before, the ppy film thickness increases from 40 nm up to 4.79 μm yielding a film 1000 times thicker. The cyclic voltammogram obtained during the preparation of such film, is presented in Fig. 5. The film morphology, based on AFM images, was found to be completely independent of the substrate characteristics. This agrees with a previous observation of Li and Wang,[19,21] for polymer films thicker than 1 μm.

At this point we can conclude that the ppy film surface morphology depends on many different parameters, which are difficult to

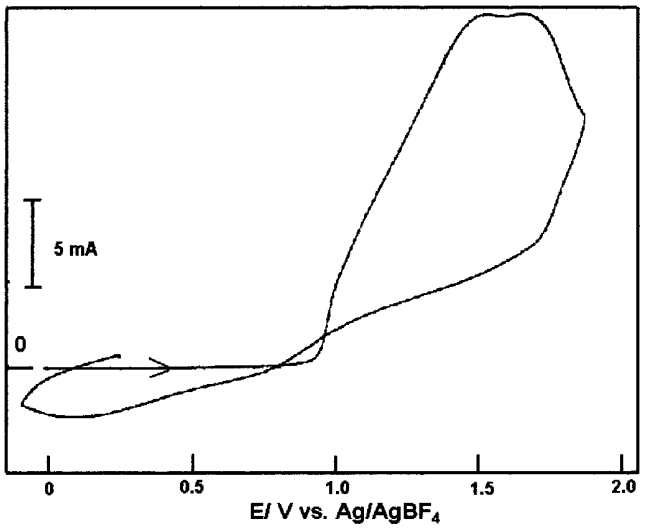


**Figure 5.** Cyclic voltammogram of Py oxidation on platinum polycrystalline film in acetonitrile solution containing 0.1 M $Et_4NBF_4$, 0.22 M of pyrrole.

control simultaneously, when the preparation is performed using a voltammetric method. Therefore, the surface morphology of thin ppy films synthesized by potential step chronoamperometry was examined using very short times of electrolysis.

*PPY film formation by the potential step method (potentiostatic method).*—According to the literature, the potential step (potentiostatic) method has been commonly used for the ppy film preparation in contrast to the voltammetric technique. In recent papers polymer surface morphology (the film thickness and the film roughness) was shown to depend on the film preparation conditions.[9,14,23-25,42] In these studies the ppy films were visualized utilizing SEM, AFM, and STM methods and the polymer films were about 1 μm thick, which means that those studies were mainly concerned with the latter stages of the polymer film growth.

In this study, effort is focused on the characterization of ultrathin ppy films (up to 50 nm thick) prepared by the potential step chronoamperometry. Films were formed from an acetonitrile solution containing 0.22 M of Py and 0.1 M $Bu_4NBF_4$ as a doping electrolyte. To initiate film growth on the Pt electrode, the potential was stepped from 0.10 to 1.30 V for different periods of time. Short potential steps (50 ms to 5 s) were used deliberately to see changes in the film morphology during the very early stages of the polypyrrole growth. All ppy films were analyzed by AFM in their oxidized state, just after the potential step experiment.

Figure 6a-c shows a set of AFM images of the ppy film surface, formed using (a) 50 ms, (b) 200 ms, and (c) 5 s pulse time, respectively. They clearly reveal that the polymer film contains small ppy clusters (nodules). After a very short potential step of 50 ms, Fig. 6, the ppy clusters (seen in the image as small light colored features) were found dispersed all over the platinum electrode. The large trenches over the sample surface are related to the platinum substrate morphology (polycrystalline Pt). When the pulse time of 200 ms is employed, the image of the platinum substrate characteristics is diminished due to the increment of deposited polymer (the surface is flat). The rough surface drops from 15.0 ± 0.2 nm for sample with 5 ms of deposition, to 11.4 ± 0.2 nm for a sample with 200 ms of deposition. Undoubtedly, the reason for such a change is the ppy film development. After 5 s (Fig. 6c), the ppy deposit already possesses a new morphology, with ppy clusters fusing to form a smooth compact film. Then the morphology is dominated by topographic characteristics of the ppy film. In order to gain more insight about the nucleation and growth process during ppy film formation, a detailed analysis of the cluster size was performed. Figure 7 shows

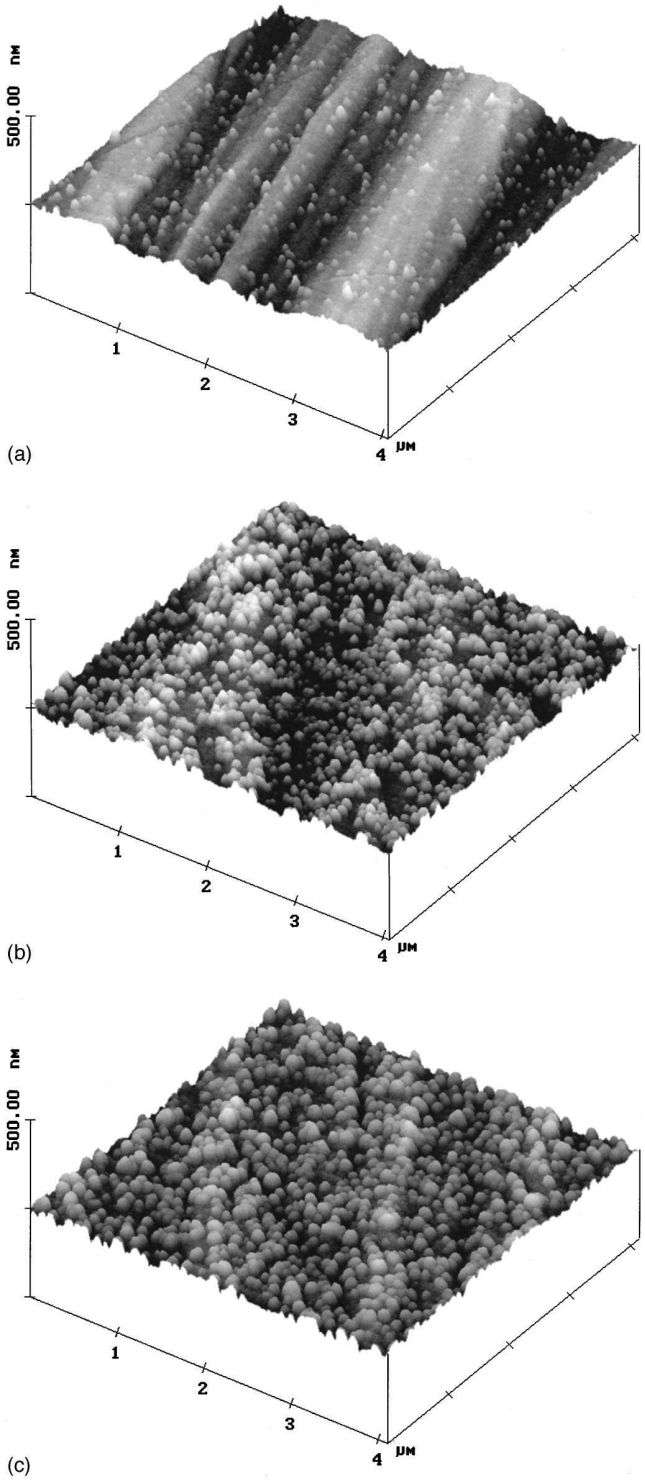


**Figure 6.** Set of AFM images show the Pt electrode surface covered by ppy polymer nodules. The film was prepared by potentiostatic method, utilizing potential pulses at 1.30 V, during different periods of time (a, top) 50, (b, middle) 200, and (c, bottom) 5 s, respectively, in acetonitrile solution containing: 0.1 M $Et_4NBF_4$ and 0.22 M Py.

a set of graphics with cross sections taken from the images presented in Fig. 6a-c. In order to compare and emphasize differences between ppy cluster sizes, the *z* scale was kept equal. It clearly illustrates that ppy clusters gain on height and width during deposition. Simultaneously, a longer deposition time results in a larger

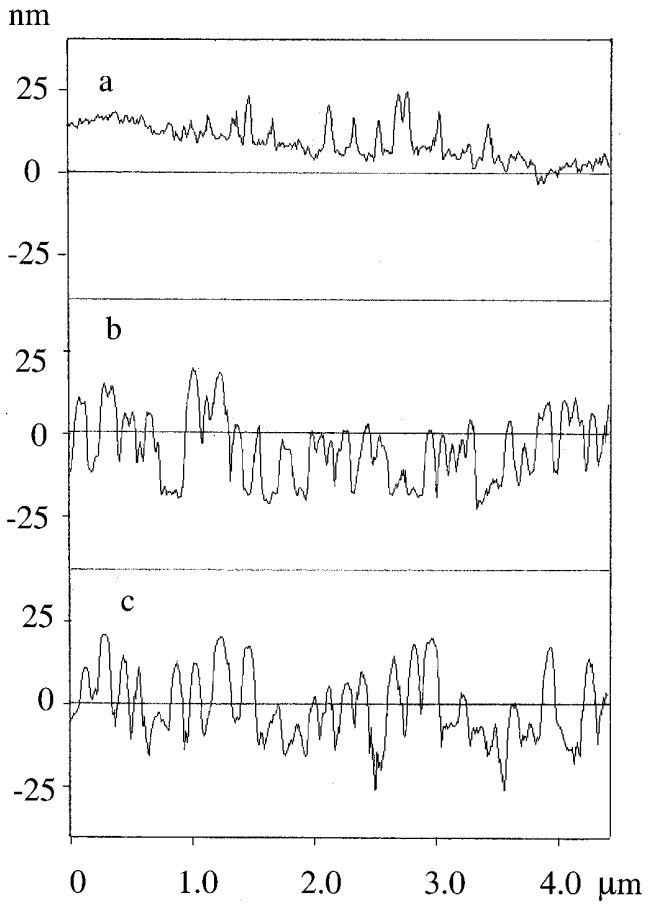


**Figure 7.** Set of cross sections taken over surface area on images of (a) Fig. 6a, (b) Fig. 6b, and (c) Fig. 6c demonstrates differences in the ppy film morphology due to different potential pulses.

number of ppy clusters on the electrode surface. Analysis of the height, diameter (width), and number of clusters per imaged area as a function of electrodeposition time is plotted in Fig. 8. At the earliest stage of the deposition process, the number of ppy clusters increases with deposition time, corresponding to progressive nucleation. Subsequently the ppy clusters grow more rapidly in height (become taller) than in width.

A comparison between voltammetric and the potential step (potentiostatic) methods clearly indicates that the latter allows better monitoring and control during the ppy film growth. In particular, the potentiostatic method afforded visualization and characterization of the early stages of ppy film development under a fixed degree of supersaturation. However, the association process between the polymer grains (nodules), regularly observed for oxidized films grown by voltammetric technique, was absent when the potentiostatic method was used. Apparently, the very short time of potential steps (low to 5 s) at which the film is exposed to positive potentials, is not sufficient to initiate the grain association process. It also indicates that kinetics of the oxidative grain association is probably very slow, then the images always showed that the ppy film consisted of individual ppy clusters maintaining their original shape, in spite of the electropolymerization progress. Therefore using the potential step method, the additional polymer transformation process involving the grain association was successfully eliminated yielding polymer films with uniform grains.

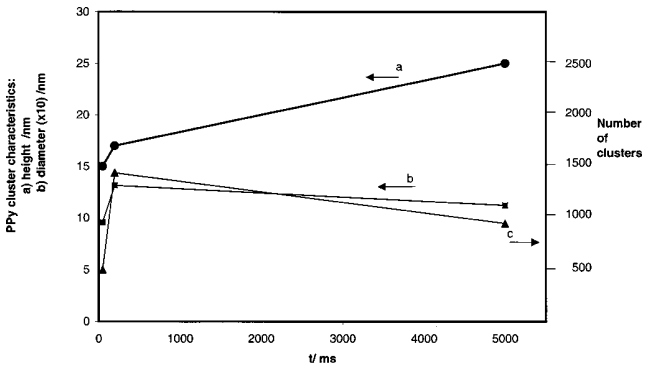


**Figure 8.** PPY cluster characteristics and dependence of electrolysis time at the potential pulses.

## Conclusions

In the reduced state, the AFM images show numerous nanosize nodules with two dominant sizes for single and double-size grains on the ppy film formed by the voltammetric method. Based on these observations we conclude that the ppy grains were formed simultaneously, which is characteristic of instantaneous nucleation. On the other hand, the oxidized ppy film surface also shows associated grains, such as a new phase, as well as an increment on the surface roughness. We suppose that this is the result of the ppy volume change, promoted by anion uptake into the polymer matrix at positive potentials. In additional experiments with different doping anions, we confirm that the ppy film morphology is unaltered if the anion exchange process (between the polymer matrix-solution interface) is avoided. The surface morphology of thicker ppy films (*ca.* 5 nm thickness) is uneffected by changes in the redox state.

The potential step method for ppy film preparation allows better growth control and visualization at very early stages of the electropolymerization process. AFM images clearly reveal the surface morphology, shape, size, and distribution of the individual polymer nodules. In addition, the evolution of the ppy growth could be easily followed. Initially, the ppy nodules are isolated and randomly distributed over the platinum electrode. During the longer potential pulses, the ppy nodules grow three-dimensionally simultaneously increasing the number of grains on the electrode surface in a progressive manner. Interestingly, during the potentiostatic growth, limited association to form larger aggregates of ppy nodules was observed, suggesting that the potentiostatic growth is a better alternative for obtaining the thin ppy films with defined smooth surface morphology.

## Acknowledgments

The research reported in this article has received financial support from CONACyT, projects 0913E-P; L0081-E9608, and the Cátedra Patrimonial de Excelencia Nivel II, for N.B. M.S. thanks DGAPA and CONACyT for financial support through the projects IN-500597 and 25267-A. T.H.P. also thanks CONACyT for the scholarship support.

*Universidad Nacional Autónoma de México assisted in meeting the publication costs of this article.*

## References

1. A. F. Díaz, J. Castillo, K. K. Kanazawa, J. A. Logan, M. Salmón, and O. Fajardo, *J. Electroanal. Chem.*, **133**, 233 (1982); T. Kobayashi, H. Yoneyama, and H. Tamura, *J. Electroanal. Chem.*, **161**, 419 (1984).
2. T. Osaka, S. Ogana, K. Naoi, and N. Oyama, *J. Electrochem. Soc.*, **136**, 306 (1989).
3. D. J. Walton, *Mater. Des.*, **11**, 142 (1990).
4. M. R. Anderson, B. R. Mattes, H. Reiss, and R. B. Janner, *Science*, **252**, 1414 (1991).
5. N. Ogura, H. Ejiri, and K. Takeishi, *J. Electrochem. Soc.*, **140**, 602 (1993).
6. A. F. Diaz and K. K. Kanazawa, *J. Chem. Soc. Chem. Commun.*, **1979**, 635.
7. A. F. Diaz, *Chem. Scr.*, **17**, 145 (1981).
8. P. A. Christensen and A. Hamnett, *Electrochim. Acta*, **36**, 1263 (1991).
9. M. F. Suares and R. G. Comptom, *J. Electroanal. Chem.*, **462**, 211 (1999).
10. A. F. Diaz, K. K. Kanazawa, and M. Salmón, *IBM Tech. Discl. Bull.*, **24**, 2381 (1981).

11. A. F. Diaz and B. Hall, *IBM J. Res. Dev.*, **27**, 342 (1983).
12. G. R. Mitchell, F. J. Davis, and C. H. Legge, *Synth. Met.*, **26**, 247 (1988).
13. R. Stankovic, O. Pavlovic, M. Vojnovic, and S. Jovanovic, *Eur. Polym. J.*, **30**, 385 (1994).
14. J. S. Shapiro, W. T. Smith, and C. MacRae, *Polymer*, **36**, 1133 (1995).
15. F.-R. F. Fan and A. J. Bard, *J. Electrochem. Soc.*, **136**, 3216 (1989).
16. R. Yang, D. F. Evans, L. Christensen, and W. A. Hendrickson, *J. Phys. Chem.*, **94**, 6117 (1990).
17. S. P. Armes, *Langmuir*, **7**, 1447 (1991).
18. R. Yang, W. H. Smyrl, D. F. Evans, and W. A. Hendrickson, *J. Phys. Chem.*, **96**, 1428 (1992).
19. J. Li and E. Wang, *Synth. Met.*, **66**, 67 (1994).
20. K. Naoi, N. Oura, M. Maeda, and S. Nakamura, *J. Electroanal. Chem.*, **142**, 417 (1995).
21. M. Salmón, A. F. Díaz, A. J. Logan, M. Krounbi, and J. Bargón, *Mol. Cryst. Liq. Cryst.*, **83**, 265 (1982).
22. A. Kaynak, *Mater. Res. Bull.*, **32**, 271 (1997).
23. T. Silk, Q. Hong, J. Tamm, and R. G. Compton, *Synth. Met.*, **93**, 59 (1998).
24. T. Silk, Q. Hong, J. Tamm, and R. G. Compton, *Synth. Met.*, **93**, 65 (1998).
25. Y. Yang, S. Mu, and H. Chen, *Synth. Met.*, **92**, 173 (1998).
26. E. Chainet and M. Billon, *J. Electroanal. Chem.*, **451**, 273 (1998).
27. K. Naoi, N. Oura, M. Maeda, and S. Nakamura, *J. Electroanal. Chem.*, **142**, 417 (1995).
28. A. F. Díaz, A. Martínez, K. K. Kanazawa, and G. P. Gardini, *J. Chem. Soc. Chem. Commun.*, **1979**, 635.
29. R. A. Bull, F.-R. F. Fan, and A. J. Bard, *J. Electrochem. Soc.*, **129**, 1009 (1982).
30. Z. Qi, N. G. Rees, and P. G. Pickup, *Chem. Mater.*, **8**, 701 (1996).
31. T. F. Otero, H. Grande, and J. Rodriguez, *J. Phys. Chem. B*, **101**, 3688 (1997).
32. M. T. McDemott, C. A. McDemott, and R. L. McCreery, *Anal. Chem.*, **65**, 937 (1993).
33. K. Jowal, L. Xie, R. Hug, and G. C. Farrington, *J. Electrochem. Soc.*, **139**, 2818 (1992).
34. R. J. Phillips, T. D. Golden, and M. G. Shumsky, *J. Electrochem. Soc.*, **141**, 2391 (1994).
35. D. Aubach and Y. Cohen, *J. Electrochem. Soc.*, **143**, 3525 (1996).
36. Y. G. Li and A. Lasis, *J. Appl. Electrochem.*, **27**, 643 (1997).
37. T. F. Otero, H. Grande, and J. Rodriguez, *J. Phys. Chem. B*, **101**, 8525 (1997).
38. T. B. Otero, H. Grande, and J. Rodriguez, *Synth. Met.*, **85**, 1077 (1997).
39. T. Shimidzu, A. Ohtani, T. Iyoda, and K. Honda, *J. Electroanal. Chem.*, **224**, 123 (1987).
40. J. Boacka, Z. Gao, A. Ivaska, and A. Lewenstam, *J. Electroanal. Chem.*, **368**, 33 (1994).
41. Y. Li, *Electrochim. Acta*, **42**, 203 (1997).
42. T. F. Otero and E. Angulo, *Solid State Ionics*, **63-65**, 803 (1993).